Acta Parasitologica (2025) 70:148
https://doi.org/10.1007/s11686-025-01087-y

RESEARCH

Characterization of Calcifying Nanoparticles Isolated and Cultured in the Outer Capsule Wall of Hepatic Hydatid Cyst and their Correlation with Autophagy

Haojie Shi[1] · Sanqiang Niu[1] · Xuanli Su[1] · Furong Xu[1] · Xiangwei Wu[1] · Hongwei Zhang[1] · Yuchang Wang[2] · Jian Yang[1,3]

Received: 18 February 2025 / Accepted: 24 June 2025

Abstract

Purpose To isolate calcifying nanoparticles (CNPs) from the outer capsule wall of hepatic hydatid cysts and determine their in vitro characteristics and potential link to autophagy-mediated inflammation.

Methods CNPs were isolated from 47 hepatic hydatid cyst walls and cultured for 4 weeks. The morphology and ultrastructure were examined using electron microscopy, and the elemental composition was determined using Energy-dispersive X-ray Microanalysis. Zeta potentials and particle size distributions were examined using a Zetasizer. The expression of autophagy-related proteins (LC3B, Beclin-1, and SQSTM1/P62) was analyzed using immunohistochemistry and western blotting.

Results CNPs derived from the outer capsule wall of hepatic hydatid cyst exhibited similar properties to those of previously reported CNPs. The expression levels of Beclin-1 and LC3B were significantly elevated in calcified compared to non-calcified cyst walls ($P<0.05$), whereas that of SQSTM1/P62 was higher in non-calcified walls ($P<0.05$). The increased Beclin-1 and LC3B expression in calcified walls and SQSTM1/P62 in non-calcified walls ($P<0.01$) were confirmed using immunohistochemistry. The content of CNPs was significantly higher in the calcified cyst walls ($P<0.001$).

Conclusions CNPs can be isolated and cultured from the outer capsule wall of hepatic hydatid cysts, They are associated with autophagic activity in the outer capsule wall tissue and calcification of the cyst wall.

Keywords Calcifying nanoparticles · Autophagy · Hepatic cystic echinococcosis · Calcification · Electron microscopy

Introduction

Hepatic echinococcosis, a parasitic disease that poses a significant threat to human and animal health, is prevalent in western agricultural and animal husbandry regions in China, such as Xinjiang, Qinghai, and Tibet. Hepatic cystic echinococcosis (HCE) constitutes > 90% of all reported echinococcosis cases [1–3]. The available treatments for hepatic echinococcosis yield limited therapeutic outcomes [4]. Indeed, pharmacological interventions have shown limited efficacy, and surgical approaches are excessively traumatic for patients and prone to recurrence. Outer capsule wall calcification does not correspond to parasite death; however, it is indicative of clinical dormancy and a loss of biological activity. The factors triggering cyst wall calcification in HCE remain contentious [5]. Promoting cyst wall calcification is a potential strategy for the treatment of HCE [6].

Haojie Shi, Sanqiang Niu contributed equally to this work and are therefore co-first authors.

✉ Jian Yang
125210525@qq.com

[1] The First Affiliated Hospital of Shihezi University, Shihezi, Xinjiang 832000, China

[2] Trauma Center, Department of Emergency and Traumatic Surgery, Tongji Hospital of Tongji Medical College, Huazhong University of Science and Technology, Wuhan, Hubei 430030, P. R. China

[3] NHC Key Laboratory of Prevention and Treatment of Central Asia High Incidence Diseases, The First Affiliated Hospital of Shihezi University, Shihezi, China

Published online: 07 July 2025

Calcifying nanoparticles (CNPs), discovered by the Finnish scientist Kajander, were initially referred to as nanobacteria and nanobacteria-like particles [7]. CNPs have been shown to induce deposition and growth of calcium phosphate salts under pathological conditions [8]. Previous studies have also established a strong association between CNPs and the development of various pathological conditions, such as calcified aortic stenosis, atherosclerosis, kidney stones, chronic prostatitis, polycystic liver disease, gallstones, placental calcification, rheumatoid arthritis, chronic periodontitis, peripheral neuropathy, and other forms of pathological calcification and chronic inflammatory diseases [8–10].

Autophagy, a common mechanism underlying programmed cell death, is triggered by environmental stressors. Cellular autophagy is amplified via signal transduction pathways stimulated by apoptosis [11]. Nicolao et al. [12] have reported that bortezomib induces autophagy and cell death in *Echinococcus granulosus* larvae by inducing endoplasmic reticulum stress. Similarly, Loos et al. [13] reported that metformin increased glycolysis and autophagy by modulating AMP-activated protein kinase activation in *Echinococcus scolices*. Additionally, CNPs can adversely affect renal tubular epithelial cells by increasing autophagic activity, thereby promoting the development and aggregation of calcium salt crystals in renal tubules, which have been linked to kidney stone formation [14–17].

Previously, Yang et al. successfully isolated and cultured CNPs from the calcified outer capsule wall of hepatic hydatid cysts, providing evidence of the presence of CNPs in this pathological condition [18]. Our initial study was the first to suggest a potential association between cyst wall calcification and CNPs in the natural progression of HCE. Consequently, we hypothesized that CNPs influence the regulation of autophagy and cyst wall calcification in cystic hepatic hydatid disease. To test this hypothesis, we isolated and cultivated CNPs derived from the outer capsule wall of hepatic hydatid cysts, characterized their growth patterns in vitro, and investigated the potential link between the inflammatory response induced by the isolated CNPs and cellular autophagy.

Materials and Methods

Patients

The inclusion criteria were (1) patients diagnosed with hepatic echinococcosis using B-ultrasound, computed tomography (CT), magnetic resonance imaging (MRI), hydatid antibodies, and other examinations before surgery, and (2) patients willing to undergo surgical treatment. Patients with alveolar hepatic echinococcosis for whom the clinical classification of hepatic echinococcosis could not be determined were excluded.

A total of 47 patients diagnosed with HCE and confirmed by surgery at our hospital between 2021 and 2024 were included in the study. The cohort consisted of 24 males and 23 females, with a median age of 45 years (ranging, 12–80 years). The clinical dataset included the general condition of the patients; epidemiological history; number, location, and size of cysts as determined by B-ultrasound or CT; WHO image classification; surgical method; type of cysts; maximum diameter of the internal and external cysts. This study was approved by the Science and Technology Ethics Committee of the First Affiliated Hospital of Shihezi University School of Medicine (Approval number: KJ2022-221-02). All experimental procedures were conducted in accordance with the relevant guidelines and regulations. Written informed consent was obtained from the research subjects included in this study.

Handling of the Specimen

Preoperative CT revealed a calcified hepatic hydatid cyst within the outer capsule (Fig. 1A), which was successfully excised during surgery (Fig. 1B). The calcified outer capsule wall of the hepatic hydatid cyst was cut into small pieces (Fig. 1C).

In total, 500 mg of calcified and non-calcified echinococcosis outer capsule walls specimens obtained from surgical specimens of patients who underwent surgical treatment were weighed, washed with sterile phosphate-buffered saline (PBS), ground into a tissue homogenate in a sterile mortar, and added to a solution of diluted hydrochloric acid (0.1 mol/L). The mixture was demineralized, the pH was adjusted to a range of 7.0–7.4 by Tris-HCl buffer solution(pH = 8), and the supernatant was collected after natural precipitation and high-speed centrifugation. The resulting solutions were passed through a 0.22-μm bacterial filter and incubated in a water bath at 56 °C for 30 min to remove contamination by mycoplasma. Subsequently, the supernatant was retrieved at low temperature and filtered through a 0.22-μm bacterial filter into a cotton plug test tube (2 mL/tube) and added to 4 mL of RPMI-1640 culture medium containing 10% γFBS. The cultivation period is approximately 4 weeks. Four replicate tubes were prepared per sample. The calcified outer capsule wall group exhibited a white flocculent precipitate at the bottom of the tube (Fig. 1D), which dissolved in the culture medium after shaking and reappeared after standing.

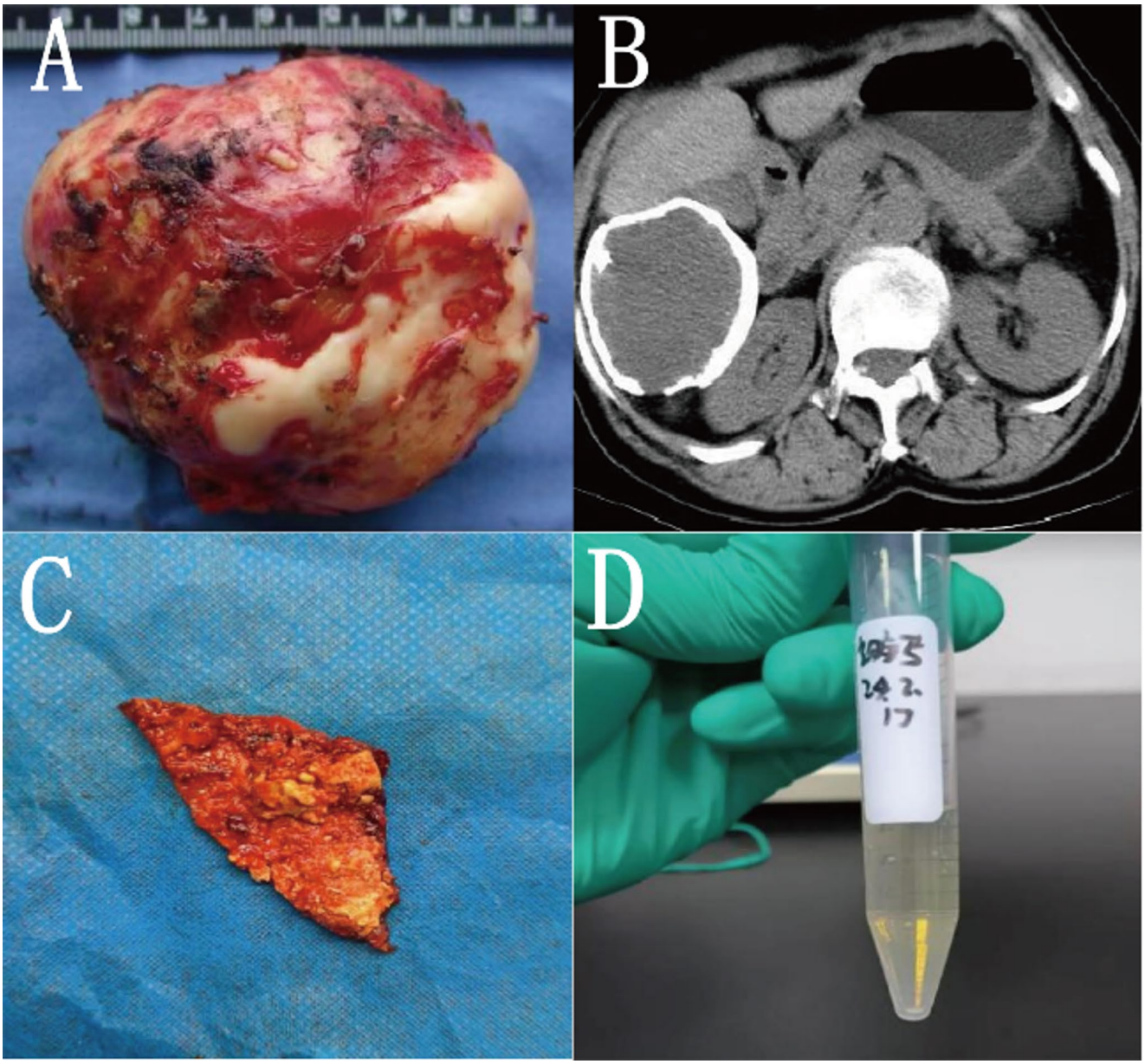

Fig. 1 Isolation and culture of calcifying nanoparticles (CNPs) from hepatic hydatid cyst walls. **A**: Calcified hepatic hydatid cyst specimen. **B**: Preoperative computed tomography image of hepatic cystic echinococcosis. **C**: Specimen cut from the calcified outer capsule wall. **D**: CNPs isolated from the hepatic hydatid cyst walls

Morphological Observations

The samples were analyzed using transmission electron microscopy (TEM) scanning. Briefly, the white flocculent precipitate obtained from the culture was centrifuged at 16,000 rpm for 30 min. The supernatant was discarded, and the precipitate was fixed with PBS buffer and 2.5% glutaraldehyde at 4 °C for 24 h. Thereafter, the precipitate was washed three times with double-distilled water for 5 min each. After centrifugation, 0.5 mL of double-distilled water was added to the suspension. A 200-mesh copper mesh with a carbon support film was floated onto a droplet of the suspension and allowed to stand for 5 min. Excess liquid was carefully removed from the copper mesh using a filter paper and allowed to dry naturally at 15–25 °C. Observations were conducted using an HT7700 TEM with an operating voltage of 80 kV.

Observation of CNPs Using Scanning Electron Microscope and Detection of their Surface Element Content

The samples were analyzed using scanning electron microscopy (SEM). Briefly, white precipitate samples obtained after high-speed centrifugation were fixed with 2.5% glutaraldehyde for 1–2 h, successively dehydrated with a range of ethanol concentrations, and frozen. The samples were subsequently observed using a SEM after plating a metal film on the surface. Typical CNPs were selected to analyze their elemental compositions via energy-dispersive X-ray microanalysis (EDX).

Particle Size Distribution and Zeta Potential Detection

An appropriate amount of the white flocculent precipitate was dissolved in pure water to create a suspension, placed in a dedicated sample container, and manually premixed using a horizontal circular motion to disperse the particles and prevent them from adhering to the container walls. Subsequently, the sample container was partially immersed in the water tank of an ultrasonic processing device. Ultrasonic equipment at a frequency of 40 kHz and power of 80 W was used for dispersion with a processing time of 20 min. The cooling water in the water tank was regularly replaced to maintain the processing temperature within t15–25 °C range to avoid temperature increases caused by energy conversion during ultrasonic processing, which can potentially affect the properties of the sample. The samples were diluted 10-fold with pure water and analyzed for particle size and zeta potential using a nanoparticle-size zeta potential analyzer.

Immunohistochemistry Analysis of LC3B, Beclin-1, and SQSTM1/P62 Expression

The expression of LC3B, Beclin-1, and SQSTM1/P62 was detected via immunohistochemistry. Calcified, non-calcified, CNP culture-positive, and CNP culture-negative external capsule tissues were selected for analysis. The samples were fixed in 10% neutral-buffered formaldehyde for 48 h, followed by routine dehydration, clearing, and embedding in paraffin. Sections were cut into 4 μm-thick slices, mounted on anti-fade slides, dewaxed with xylene in water, and underwent antigen retrieval using citrate buffer (pH 6.0). The sections were heated to a boil in a microwave oven, maintained for 10 min, and cooled naturally to 15–25 °C. The sections were incubated overnight at 4 °C with a primary antibody, with a dilution factor of 1:100. Subsequently, the sections were incubated with a horseradish peroxidase-labeled goat anti-mouse IgG secondary antibody, diluted at 1:200, at room temperature for 30 min. Thereafter, 3,3'-diaminobenzidine (DAB) was used as the chromogenic substrate, with the color development reaction lasting 5 min, followed by light counterstaining with hematoxylin to contrast the cell nuclei. After staining, the sections were dehydrated with graded ethanol, cleared, and mounted.

Two pathologists, working independently and unaware of each other's identities, reviewed the images. Positive expression was determined by the presence of uniform brown granules in the cytoplasm. A composite score was calculated based on the staining intensity and proportion of positive cells. Five fields of view were randomly selected for observation under a high-power microscope. The percentage of positive cells was scored according to the following criteria: a score of 1 was assigned if the percentage was $<25\%$, 2 if between 25 and 49%, and 3 if $\geq 50\%$. The degree of staining was evaluated according to the following scoring system: a score of 0, no staining; 1, gray–yellow; 2, golden; 3, brown staining. The total score for the two aforementioned indicators was then combined, with a score of 0–2 indicating a negative result, and a score of 3 indicating a positive result.

Western-Blot Analysis of LC3B, Beclin-1 and SQSTM1/P62 Expression

The selected calcified and non-calcified tissues of the outer capsule were minced, washed with PBS, and placed in grinding equipment in a low-temperature environment. The ground tissue samples were placed in an ice-cold mixture of RIPA lysis buffer, a protease inhibitor cocktail (containing phenylmethanesulfonyl fluoride 1 mM, aprotinin 1 μg/mL, and leupeptin 1 μg/mL), and phosphatase inhibitors (NaF 1 mM and Na_3VO_4 1 mM) to prevent protein degradation and dephosphorylation. Subsequently, the samples were placed in an ultrasonic cell disruptor (power of approximately 200 W and operating frequency of 20–25 kHz). The ultrasonic time was set to 3 s each time, with a 3-s interval between each cycle, for a total operating time of 1–3 min at 0–4 °C to ensure complete lysis. The lysed tissue suspension was centrifuged at 16,000 rpm for 15 min at 4 °C. The supernatant collected was the total protein extract. Protein concentration was quantitatively analyzed using the bicinchoninic acid assay to ensure consistency in protein loading in subsequent experiments.

The proteins were then separated using 12% sodium dodecyl sulphate polyacrylamide gel electrophoresis and transferred to a polyvinylidene fluoride membrane. After blocking with skim milk powder, primary antibodies (LC3B 1:1,000, Beclin-1 1:1,000, and SQSTM1/P62 1:1,000) were added, and the samples were incubated at 15–25 °C. Protein bands were detected using enhanced chemiluminescence.

Western blot images were scanned and analyzed using the UVP gel image processing system LabWorks4.6 software. The gray value of the target band was divided by that of the internal reference, β-actin, to obtain the relative expression level of the target protein.

Statistical Analysis

Data were analyzed using the statistical software package SPSS 23.0 and are expressed as the means ± standard deviations. The data were tested for normality and homogeneity of variance. An independent sample test was employed to compare the two groups, with $P<0.05$ indicating statistical significance. A chi-square test was employed, with $P<0.05$ indicating statistical significance, to compare count data between groups.

Results

The Calcified Outer Capsule Wall of the Hepatic Hydatid Cyst is Likely to Extract Calcifying Nanoparticles

Among the 47 patients with HCE, 28 exhibited calcification within the outer capsule wall, of which 19 (67.86%) demonstrated potential for culturing with CNPs. The culture of CNPs was successful in only 2 specimens without calcification in the external capsule wall of the 19 specimens, representing a success rate of 10.53%. A significant difference was observed between the two groups ($\chi^2 = 15.052$, $P<0.001$) (Table 1). The data demonstrated a significant correlation between the calcification of the external capsule wall and the occurrence of CNPs in patients with HCE.

CNPs Exhibit Diverse and Irregular Morphologies

TEM was employed to examine the ultrastructure of the white powder-like precipitate, which was composed of nanoparticles. The nanoparticles had diverse and irregular shapes, with the most frequently observed morphologies being gourds, dumbbells, beans, and rounds. The particle diameter range was 150–600 nm. The particles appeared as black high-density shadows at the center and low-density burrs in the surrounding area. Some particles were in binary division and proliferation (Fig. 2A and B). The central portion of the particles exhibited a gradual depression; their contents were divided into two distinct entities that subsequently underwent equal division, resulting in the formation of two particles similar in nature and size to the original particles (Fig. 2C and D).

Table 1 Comparison of the incidence of external cyst wall calcification and calcifying nanoparticles (CNPs) isolation and culture of hepatic cystic echinococcosis (HCE)

Hepatic hydatid cyst		Isolation and culture of CNPs		χ2	*P*
		Positive	Negative		
External capsule wall	Calcification	19 (67.86%)	9 (32.14%)	15.052	<0.001
	non-Calcification	2 (10.53%)	17(89.47%)		
	Total	21	26		

The powder samples obtained from the culture were observed and analyzed using a SEM (Fig. 3). Most particles were clustered and densely arranged (Fig. 3A), whereas only a few were scattered (Fig. 3B). The particles had uneven and cauliflower-like surfaces, with diameters of 100–600 nm. The morphological distribution of the particles was similar to that observed using TEM, with the majority exhibiting a spherical shape (Fig. 3C) and a split appearance (Fig. 3D).

The elemental composition of the surface was analyzed using EDX (Fig. 4A and B). The results indicated that the predominant elemental components of the CNPs were carbon (C), oxygen (O), calcium (Ca), and phosphorus (P). Further elemental analysis revealed that Ca constituted 25.5% of the total content, whereas O and P accounted for 61.56% and 7.22%, respectively. By weight, Ca accounted for 17.56%, O for 56.48%, and P for 12.83% (Table 2). These findings indicate that the primary elements of the CNPs are calcium phosphate and calcium carbonate salts.

The CNPs had particle sizes between 120 and 470 nm, with the peak particle size being approximately 180 nm. Potential detection suggested that the CNPs had a negative potential of −24.38 ± 0.88 mV (Figs. 5 and 6).

LC3B and Beclin-1 Expression Levels were Significantly Elevated in Calcified Cyst Wall Tissue Compared with Non-Calcified Cyst Wall Tissue, While SQSTM1/P62 Expression was Markedly Higher in Non-Calcified Hepatic Hydatid Cyst Wall Tissue

Western blotting was used to measure the expression of autophagy proteins in the calcified and non-calcified cyst wall groups. The results showed that the expression levels of LC3B and Beclin-1 in calcified cyst wall tissue were significantly higher than those in non-calcified cyst wall tissue.

Additionally, the expression level of SQSTM1/P62 was significantly higher in the non-calcified hepatic hydatid cyst wall tissue than in the calcified hydatid cyst wall tissue ($P<0.05$).

Subsequently, western blotting was used to qualitatively (Fig. 7A) and quantitatively (Fig. 7B) identify the three autophagy-related proteins in the cyst walls of patients with hepatic echinococcosis.

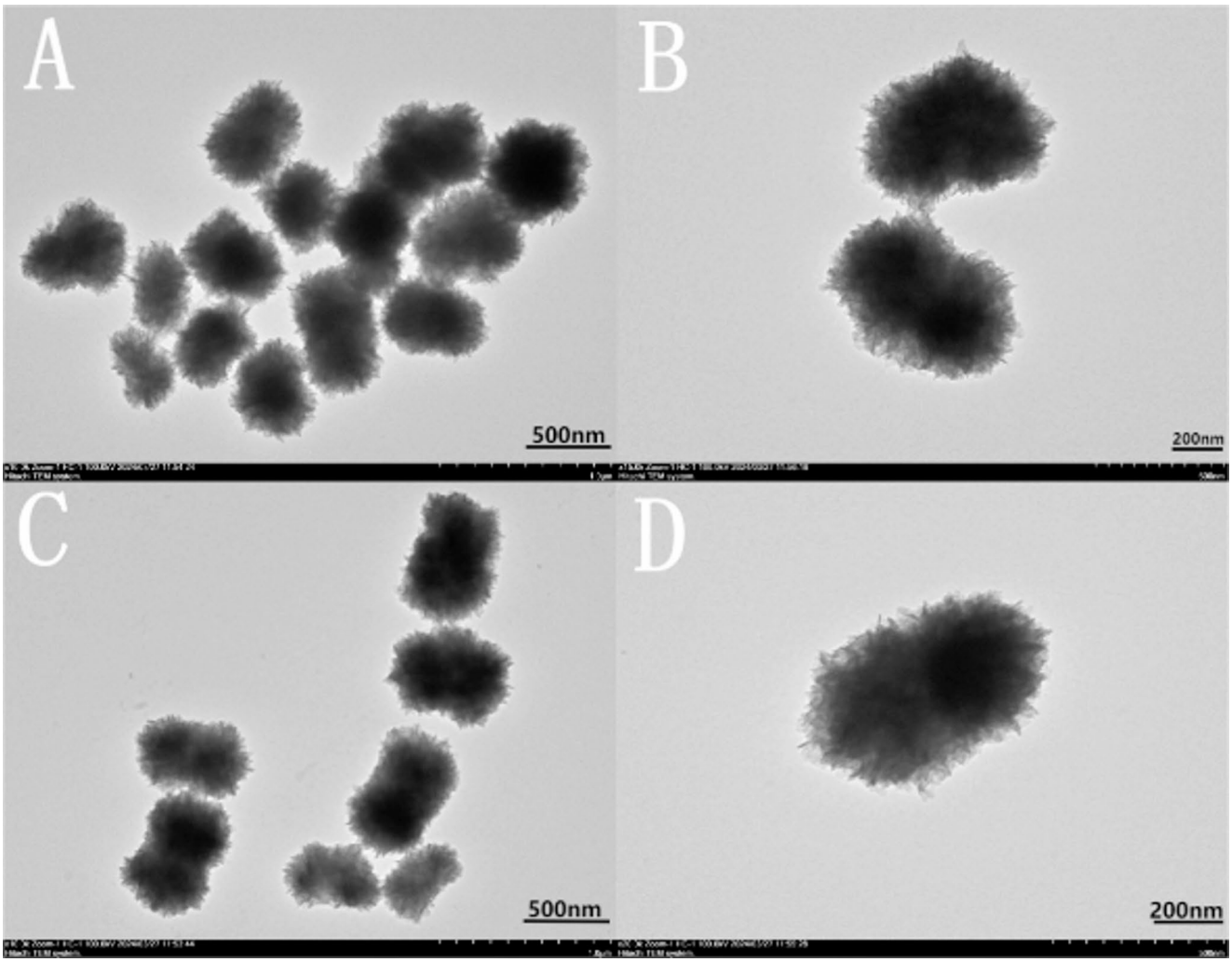

Fig. 2 Transmission electron micrographs of calcifying nanoparticles isolated from hepatic hydatid cyst walls. **A**: 10 × 100 mv; **B**: 15 × 100 mv; **C**: 10 × 100 mv; **D**: 20 × 100 mv

The expression of autophagy proteins in each group was detected using immunohistochemistry (Figs. 8, 9 and 10). Among the 47 cases of HCE, 28 had 71.43% (20/28), 78.58% (22/28), and 32.14% (9/28) expression rates of Beclin-1, LC3B, and SQSTM1/P62, respectively, in the calcified outer cyst wall. The positive expression rates of Beclin-1, LC3B, and SQSTM1/P62 in the 19 non-calcified cyst wall tissues were 31.58% (6/19), 36.84% (7/19), and 68.42% (13/19), respectively. These rates exhibited significant intergroup differences (χ^2 = 1.272, 8.341, and 5.983; $P<0.01$, 0.01, and 0.05, respectively). The expression rates of Beclin-1, LC3B, and SQSTM1/P62 in 21 CNP-positive tissues were 80.96% (17/21), 85.71% (18/21), and 14.29% (3/21), respectively. The positive expression rates of Beclin-1, LC3B, and SQSTM1/P62 in 26 CNPs-isolated and cultured negative tissues were 34.62% (9/26), 42.31% (11/26), and 90.48% (19/21), respectively. These rates exhibited notable intergroup discrepancies (χ^2 = 10.091, 9.263, and 16.127; all $P<0.01$) (Table 3).

Discussion

Discovery and Characteristics of CNPs

CNPs were discovered serendipitously by Finnish scientist Kajander [7] while investigating bovine serum culture failure. These nanoparticles, predominantly round or rod-shaped, are prevalent in various natural tissues of the human body and have diameters ranging from 100 to 600 nm. CNPs displayed physicochemical stability, including acid and heat resistance and limited susceptibility to metabolic degradation. CNPs represent self-replicating nanoscale protein complexes with inherent self-mineralization properties [19]. At the physiological levels of Ca and P, CNPs generate

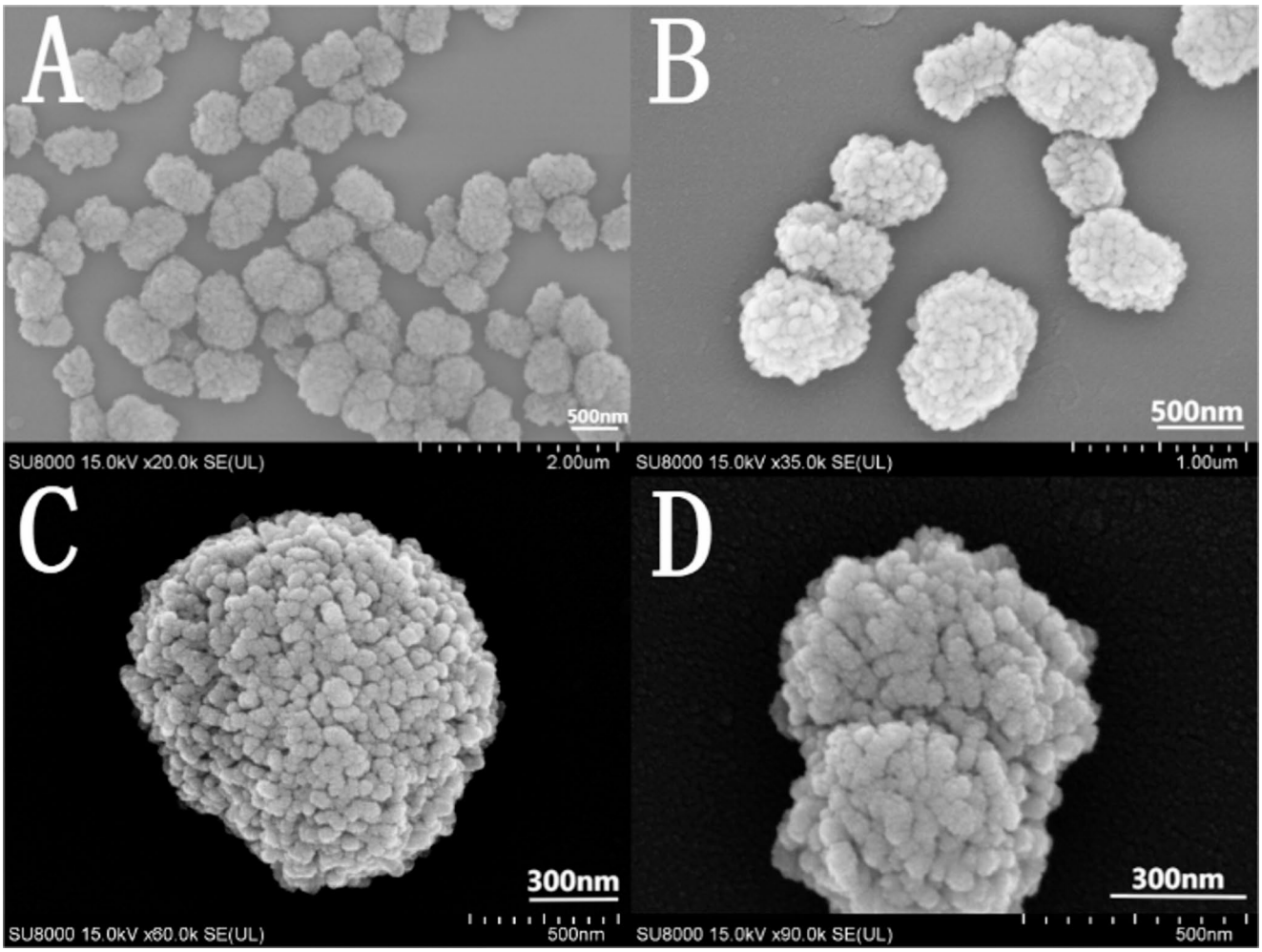

Fig. 3 Scanning electron micrographs of calcifying nanoparticles isolated from hepatic hydatid cyst walls. **A**: 20 × 15 kv × 20 k; **B**: 35 × 100 mv, 15 kv × 35 k; **C**: 60 × 15 kv × 60 k; **D**: 90 × 100 mv, 15 kv × 90 k

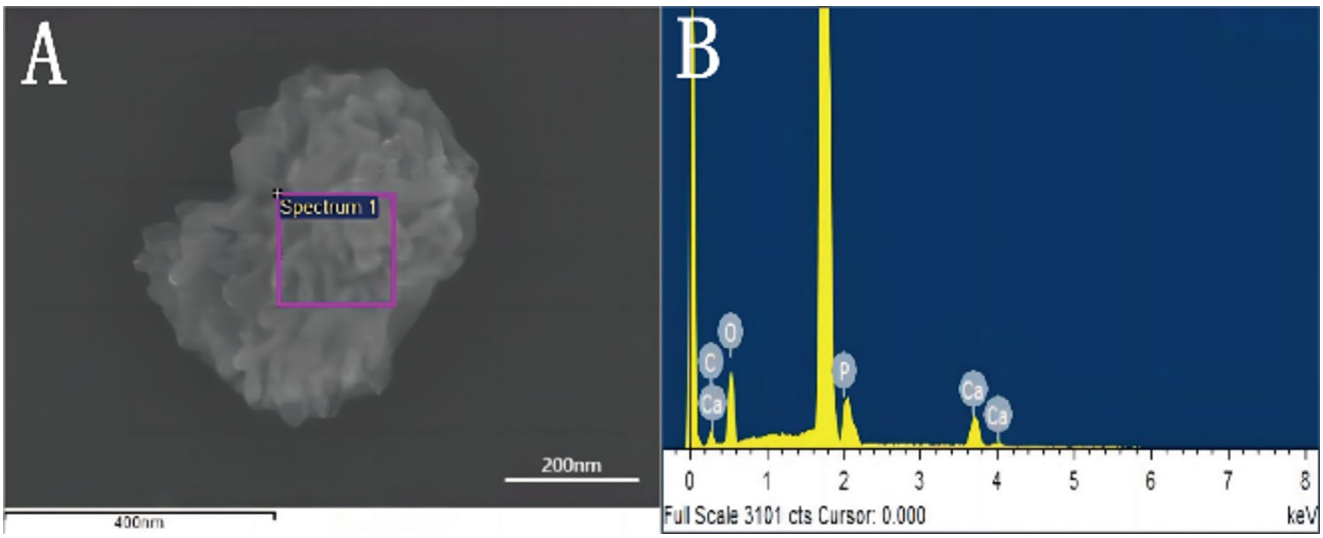

Fig. 4 Energy-dispersive X-ray microanalysis (EDX) measurement of elemental content in calcifying nanoparticles (CNPs) and measurement of X-ray energy spectrum. **A**: EDX measurement of elemental content in CNP, **B**: EDX X-ray energy spectrum of CNPs

Table 2 Predominant elemental compositions of the calcifying nanoparticles

Element	Weight%	Atomic%
C	17.56	25.5
O	56.48	61.56
P	12.83	7.22
Ca	13.13	5.71
Totals	100	100

hydroxyapatite carbonate crystals, forming a sturdy mineralized shell that encases the surroundings and forms a core crystal. Additionally, they can excrete calcified lipopolysaccharide biofilms with significant toxicity and potentially induce cell vacuolation, tissue inflammation, swelling, and trigger a cascade of associated inflammatory mediators. This establishes a close association with human pathology and infectious calcification disorders.

Isolation, Culture, and Characterization of CNPs from the Calcified Outer Capsule Wall of Hepatic Hydatid Cyst

We have previously isolated and cultured CNPs from the calcified outer capsule walls of hepatic hydatid cysts, confirming the presence of calcifying nanoparticles within the calcified outer capsule walls of the hepatic hydatid cyst [20]. In this study, we isolated and cultured CNPs from calcified outer capsule walls of hepatic echinococcosis cysts. The nanoparticles were confirmed to be CNPs; their in vitro

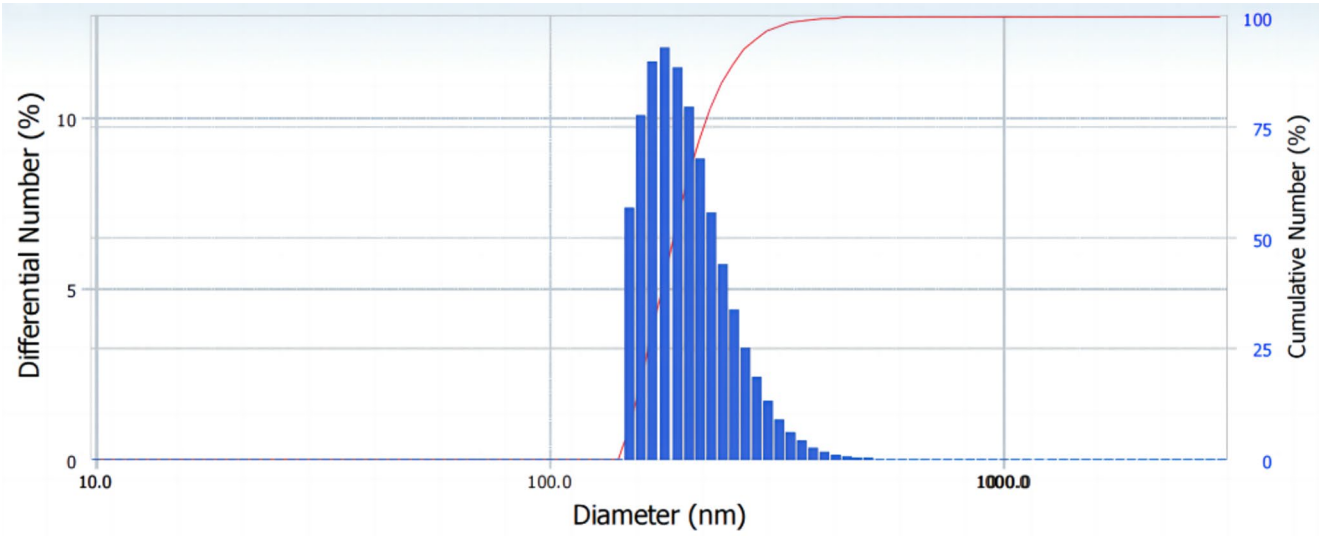

Fig. 5 Particle size distribution diagram of calcifying nanoparticles

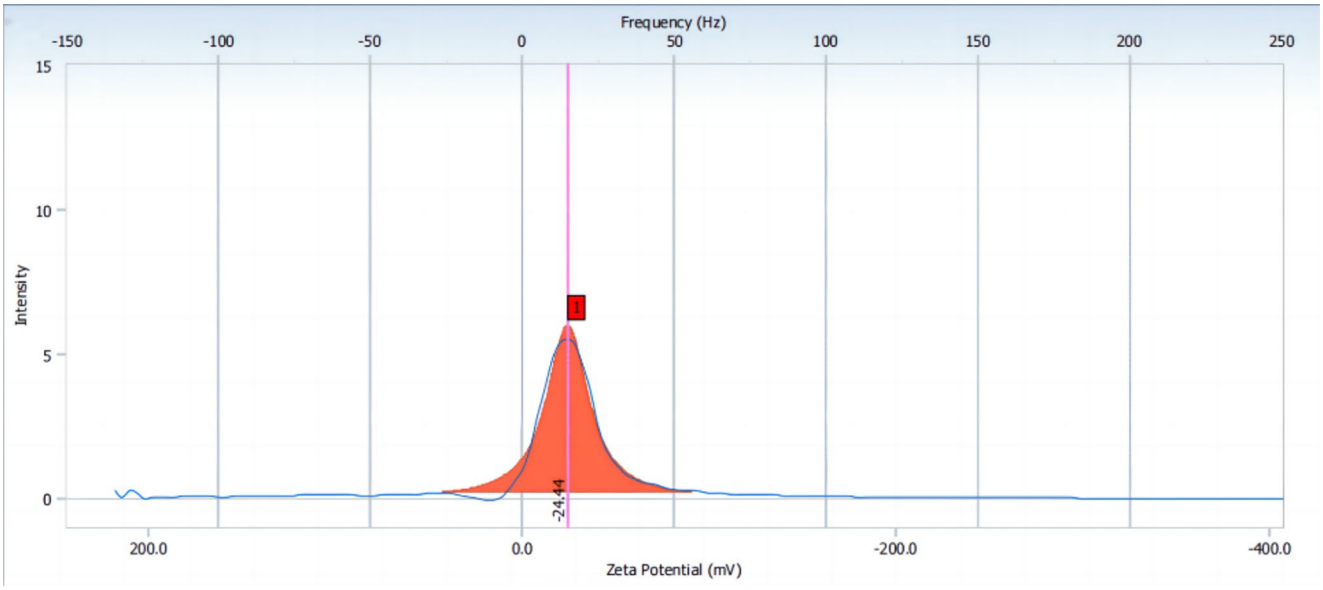

Fig. 6 Zeta potential diagram of calcifying nanoparticles

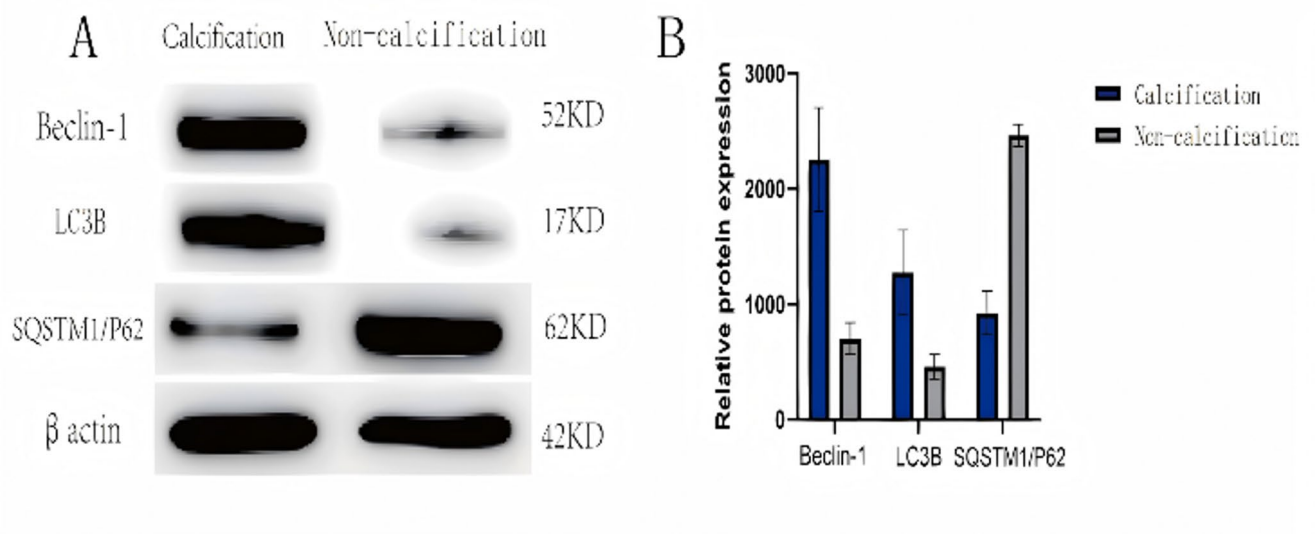

Fig. 7 Expression of autophagy-related proteins Beclin-1, LC3B, and SQSTM1/p62 using western blot. **A**: Western blot protein band diagram. **B**: Bar chart of the gray value of the western blot bands. *$P<0.001$, **$P<0.001$, ***$P<0.001$

growth characteristics were observed using electron microscopy. The surface morphological characteristics of the CNPs were consistent with those previously reported, exhibiting a crystal-like complex with irregular shapes, some of which appeared to be split with a clustered distribution. The particle size distribution was predominantly within the range of 140–470 nm, with a peak at 180 nm and a negative charge potential. After extending the cultivation cycle to 3 months, a significant increase in the white precipitate at the bottom of the culture medium was observed.

Particularly, the number and distribution density of CNPs in the field of electron microscopy significantly increased, whereas the proportion of particles exhibiting split shapes decreased. This led us to speculate that CNPs could exist in a split state under specific conditions, where the two resulting particles share similar and stable shapes, although having limited proliferation potential. Over time, the number of actively proliferating particles decreased, possibly due to variations in the volume of the culture vessel, nutrient composition in the medium, and the gaseous environment, all of which influence the microenvironment for their growth [21].

Furthermore, SEM and EDX revealed that the CNPs were primarily composed of surface elements, such as C, O, Ca, and P. This suggests that Ca and P gradually accumulate through surface charge interactions or specific chemical groups during the culturing process, leading to continuous mineralization of the particles until reaching dynamic equilibrium, thereby maintaining a stable particle morphology and characteristics.

Role of CNPs in Pathological Calcification and the Mechanisms Underlying Autophagy

In the host liver tissue, *Echinococcus granulosus* infection induces autophagy and focal calcification reactions, whose biological mechanisms may involve complex interactions between the host and parasite [22]. After recognizing *Echinococcus cysticercus* antigens, the host upregulates key autophagy-related proteins, such as LC3B, Beclin-1, and SQSTM1/p62, through the AMPK/mTOR pathway to initiate cellular autophagy, thereby degrading intracellular pathogen components and regulating immune homeostasis. This response is an important component of the host's innate immune defense. In contrast, echinococcus can interfere with host autophagy pathways through its secreted products (such as exosomes and small RNAs), potentially by delaying SQSTM1/p62 degradation and maintaining LC3B expression, among other mechanisms, to regulate the autophagy flux, thereby reducing cell necrosis and inflammation and providing a stable immune "exemption" environment for the cyst. Additionally, while cyst calcification in the late stages of infection has traditionally been viewed as the final mechanism of the host for restricting parasite survival, clinical imaging and pathological studies have revealed that some calcified cysts retain metabolic activity, suggesting calcification as an adaptive strategy for parasites to evade immunity and prolong survival by inducing local mineralization barriers [23].

In summary, autophagy and calcification may not only be host-driven immune clearance mechanisms but also exploited by parasites to promote long-term survival and maintain cyst stability.

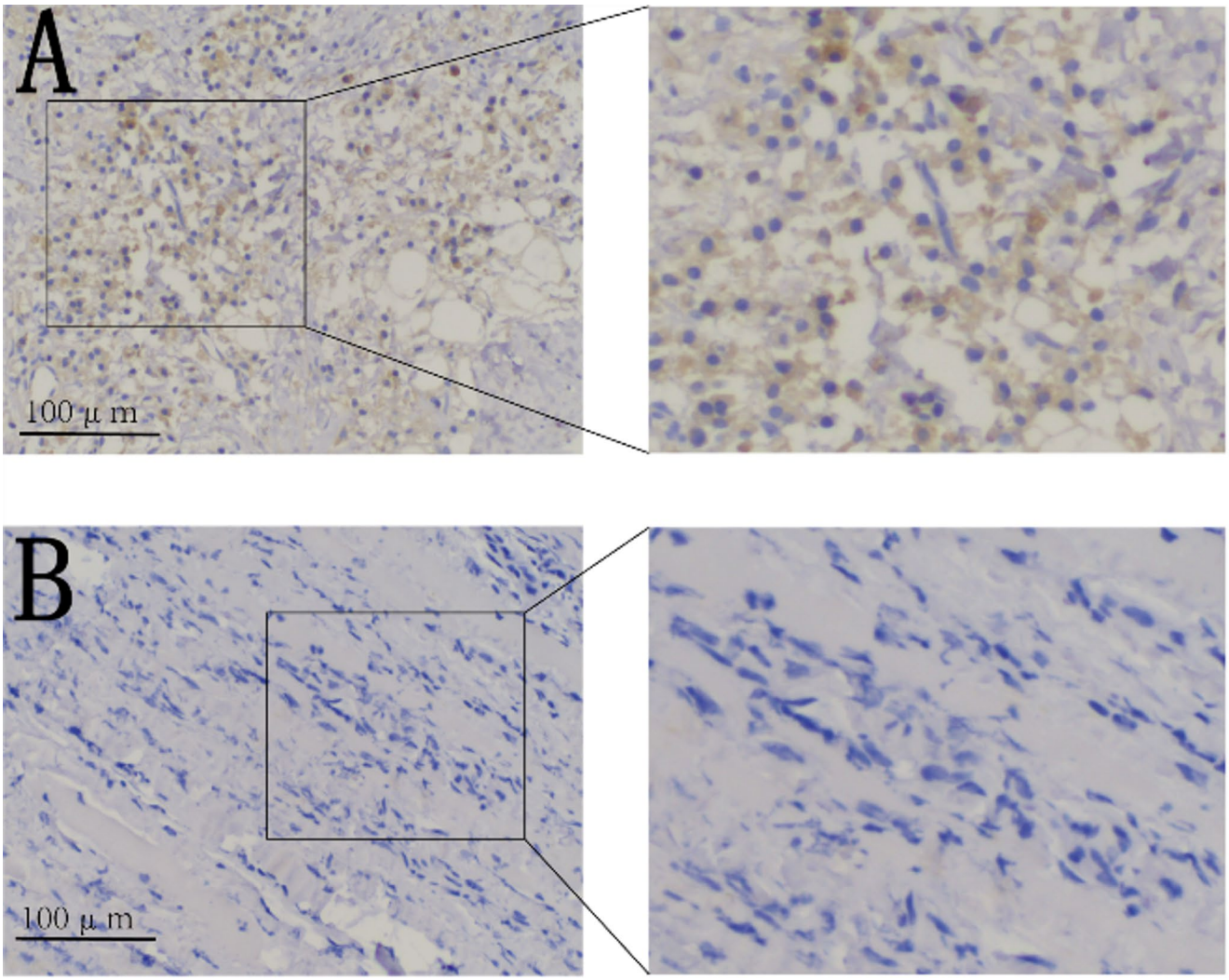

Fig. 8 Immunohistochemistry showing the Beclin-1 protein expression in the outer capsule wall of two groups of hepatic hydatid cyst. **A**: Calcified group 100 × and 400 ×. **B**: Non-calcified group 100 × and 400 ×

CNPs play crucial roles in the initiation of pathological calcification. Our previous study revealed a potential correlation between CNPs and calcification of the hydatid cyst walls in the natural progression of HCE [20]. However, the precise mechanism through which CNPs mediate calcification remains controversial. Autophagy is a common mechanism of programmed cell death activated in response to environmental stress. Nicolao et al. [12] have demonstrated that bortezomib induces autophagy and cell death in *Echinococcus granulosus* larvae via endoplasmic reticulum stress. Loos et al. [13] have reported that metformin increases glycolysis and autophagy by modulating AMP-activated protein kinase activation in echinococcosis scolices. Moreover, Hunter [24] reported that exogenous CNPs were internalized by aortic smooth muscle cells in vitro, leading to the accumulation of smooth muscle-derived apoptotic bodies at mineralized sites and increased vascular calcification. Consequently, we postulated that CNPs might influence autophagic activity and calcification of the hepatic hydatid cyst walls.

Beclin in complex with VPS34 and Atg14 initiates autophagy [25–28]. Its expression positively correlates with autophagic activity, and its overexpression enhances autophagy progression. In this study, Beclin-1 expression positively correlated with calcium content and RUNX2 protein expression in the context of vascular calcification. Additionally, autophagosome maturation is marked by LC3B, generated by dual ubiquitination of LC3. Thus, LC3B levels are key indicators of autophagic activity, with increasing levels indicating increased autophagy. In contrast, SQSTM1/P62 is a receptor protein that recognizes and removes protein aggregates. This protein binds to polyubiquitin chains and links them to LC3, connecting the cargo to autophagic structures.

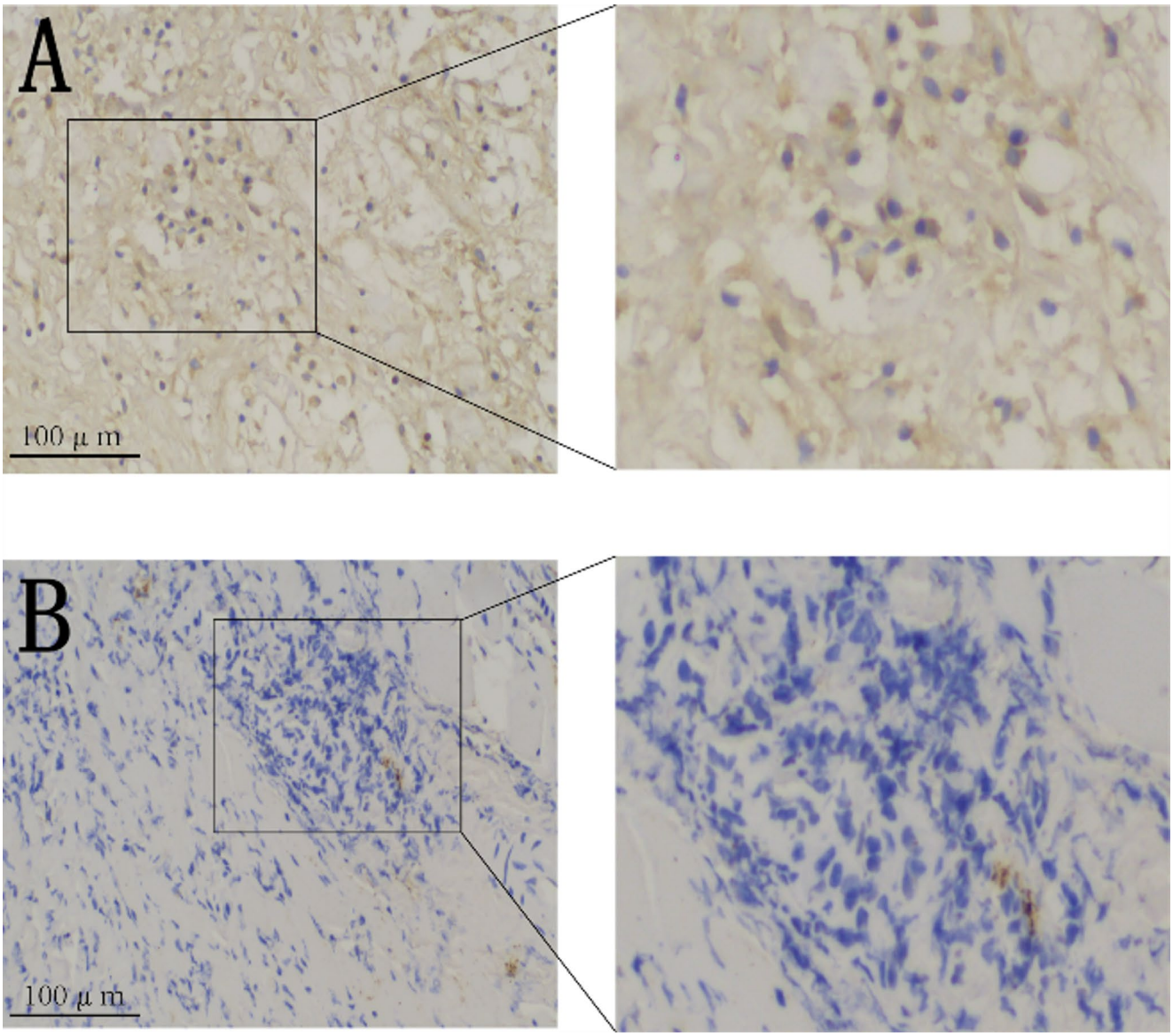

Fig. 9 Immunohistochemistry showing the LC3B protein expression in the outer capsule wall of two groups of hepatic hydatid cyst. **A**: Calcified group 100 × and 400 ×. **B**: Non-calcified group 100 × and 400 ×

SQSTM1/P62 expression levels negatively correlated with autophagic activity; SQSTM1/P62 expression increased as autophagic activity was inhibited.

Differences in Protein Expression and Autophagic Activity in Tissues and the Correlations Between CNPs and Autophagy

Our findings revealed higher expression of Beclin-1 and LC3B in the calcified outer capsule wall tissue than in the non-calcified tissue. Conversely, the positive expression rate of SQSTM1/P62 was significantly higher in the non-calcified outer capsule wall tissue than in the calcified tissue ($P<0.01$, 0.01, and 0.05, respectively). Similarly, the protein expression trends of Beclin-1, LC3B, and SQSTM1/P62 in non-calcified cyst wall tissues mirrored those in calcified tissues, indicating increased autophagy in calcified cyst wall tissues. Moreover, previous research has demonstrated a positive correlation between Beclin-1 and LC3B protein expression levels and aortic calcium content, as well as between Beclin-1 and RUNX2 protein expression in patients with chronic kidney disease, suggesting the potential role of Beclin-1 and LC3B in promoting vascular calcification through autophagy [17, 29–31]. Chengwen et al. [32] proposed that advanced glycation end-products could stimulate human aortic vascular smooth muscle cell calcification by inducing autophagy. In summary, CNPs may

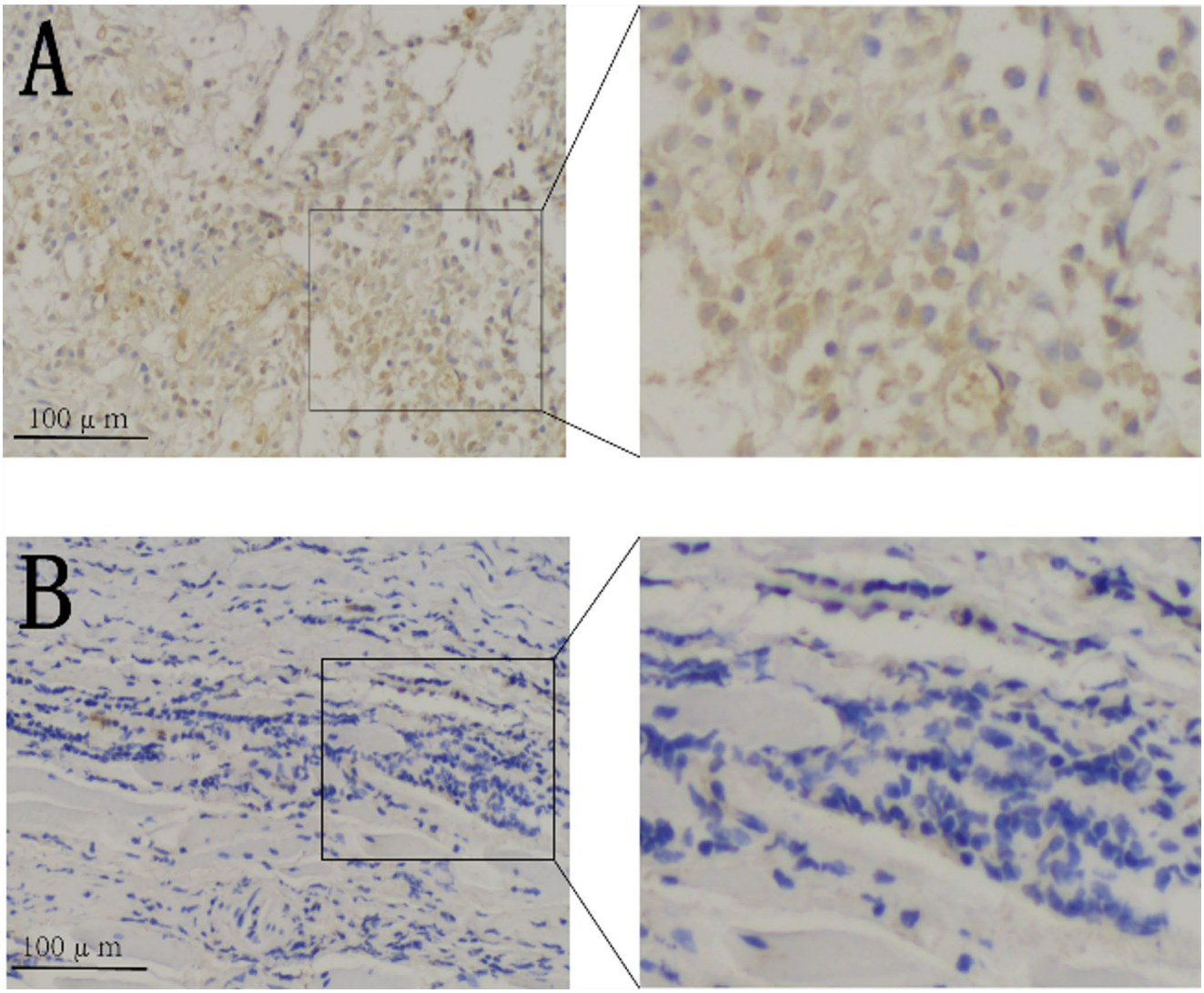

Fig. 10 Immunohistochemistry showing the SQSTM1/p62 protein expression in the outer capsule wall of two groups of hepatic hydatid cyst. **A**: Non-calcified group, 100 × and 400 ×; **B**: Calcified group, 100 × and 400 ×

induce autophagy to facilitate calcification of the outer capsule wall.

Furthermore, Beclin-1 and LC3B were significantly more highly expressed in cyst wall tissue capable of isolating and culturing to produce CNPs than in cyst wall tissue incapable of isolating and culturing to produce CNPs, while SQSTM1/P62 was more highly expressed in cyst wall tissue incapable of isolating and culturing to produce CNPs ($\chi 2 = 10.091, 9.263, 16.127$; all $P < 0.01$).

These findings suggested a correlation between CNPs and autophagy. Jianhe et al. proposed that CNPs could activate the ROS-JNK signaling pathway to increase autophagy in HK-2 cells, potentially contributing to the development of diseases associated with biomineralization, such as kidney stones. Xin reported that Beclin-1 and LC3B expression levels progressively increased following CNPs injection in rats, peaking at 24 h post-injection, and subsequently declining. This indicates that CNPs may adversely affect renal tubular epithelial cells, trigger immediate autophagy, and increase the expression of autophagy-related proteins and autophagosomes [15]. Furthermore, CNPs facilitate the formation and aggregation of calcium salt crystals in renal tubules, to some extent. Therefore, CNPs may play a role in inducing autophagy and promoting calcification in various tissues and organs.

Isolation and Culture Results of CNPs

In this study, most of the calcified cyst wall tissues could be isolated and cultured to produce CNPs (19/28), whereas most of the non-calcified cyst wall tissues could not (2/19) ($\chi 2 = 15.052$, $P < 0.001$), demonstrating that the presence of

Table 3 Expression of autophagy-related genes Beclin-1, SQSTM1/p62, and LC3B in patients with HCE with different clinical characteristics

Clinical features		Beclin-1		$\chi 2$	P	LC3B		$\chi 2$	P	P62		$\chi 2$	P
		Positive	Negative			Positive	Negative			Positive	Negative		
Sex	Male	15	9	1.023	0.312	16	8	0.512	0.474	8	16	3.577	0.059
	female	11	12			13	10			14	9		
Age (years)	≤30	7	4	-	0.342	8	3	-	0.522	5	6	-	0.915
	>30 and ≤60	17	12			18	11			13	16		
	>60	2	5			3	4			4	3		
External capsule wall	Calcification	20	8	1.272	0.007	22	6	8.341	0.004	9	19	5.983	0.014
	Non-calcification	6	13			7	12			13	6		
CNPs were isolated and cultured	Positive	17	4	10.091	0.001	18	3	9.263	0.002	3	18	16.127	0.000
	Negative	9	17			11	15			19	7		

Note: - denotes Fisher's exact probability method; CNPs, calcifying nanoparticles

CNPs was related to the pathological calcification of hepatic hydatid cysts.

In conclusion, the findings of this study indicate that CNPs are related to the expression of autophagic activity in the outer capsule tissue of patients with HCE and cyst wall calcification; that is, CNPs can induce autophagy, promoting calcification of the outer capsule wall.

Acknowledgements We express our sincere gratitude to the patients and their family members for their participation in this study.

Author Contributions (I) Conception and design: Jian Yang, Haojie Shi, and Sanqiang Niu; (II) Administrative support: Jian Yang, Xiangwei Wu; (III) Provision of study materials or patients: Haojie Shi, Sanqiang Niu, and Hongwei Zhang; (IV) Collection and assembly of data: Xuanli Su and Furong Xu; (V) Data analysis and interpretation: Sanqiang Niu, Haojie Shi, Furong Xu, Yuchang Wang, and Hongwei Zhang; (VI) Manuscript writing: All authors; (VII) Final approval of manuscript: All authors. The authors are accountable for all aspects of the work and ensure that questions related to the accuracy or integrity of any part of the work are appropriately investigated and resolved.

Funding This study was supported by the following funders:
1. Corps Directed Science and Technology Program, 2022ZD090, Preliminary Exploration and Research on the Factors Influencing the Natural Course of Cystic Liver Borreliosis.
2. Corps Science and Technology Program Project-Young Science and Technology Innovative Talents 2023CB008-31, Study on the mechanism of calcification of cysticercus hepaticus outer capsule wall due to cell autophagy induced by calcifying nanoparticles through the TGF-β/Smad pathway (Basic Research).
3. The First Affiliated Hospital of Shihezi University, Doctoral Program, BS202207, Calcifying Nanoparticles Activate TGF-β/Smad Signaling Pathway to Mediate Autophagy and Calcification of Bone Marrow Mesenchymal Stem Cells.
4. CZ001219/Bing Finance Bank [2024] No. 97-2024 Talent Development Fund-Tianshan Yingcai (the second batch) Fund for Young and Middle-aged Talents in Medicine and Healthcare.
5. National Health Commission Central Asia High-Incidence Disease Prevention and Control Key Laboratory (Co-built) Open Project Establishment Item for 2024, KF202405, "Research on the Mechanism of Calcification of Bone Marrow Mesenchymal Stem Cells Promoted by CNPs-Induced Necroptosis through the TGF-β1/TAK1/RIP3 Pathway."

Data availability statement The data supporting the findings of this research are accessible on Figshare and can be accessed at https://figshare.com/s/265b633c978877e1867c.

Declarations

Ethical Approval This study was approved by the Science and Technology Ethics Committee of the First Affiliated Hospital of Shihezi University School of Medicine (Approval number: KJ2022-221-02). All experimental procedures were conducted in accordance with the relevant guidelines and regulations. Written informed consent was obtained from the research subjects included in this study.

Disclosure The authors declare that the research was conducted in the absence of any commercial or financial relationships that could be construed as a potential conflict of interest.

Competing Interests The authors declare no competing interests.

References

1. Peng XY, Zhang SJ, Wu XW, Zhang HW, Yang J, Li J (2023) The natural decline and death course of hepatic cystic echinococcsis. Chin J Digest Surg 22:219–225. https://doi.org/10.3760/cma.j.cn115610-20221225-00713
2. Qian M, Zhou XN (2018) Walk together to combat echinococcosis. Lancet Infect Dis 18:946. https://doi.org/10.1016/S1473-3099(18)30466-3
3. Deplazes P, Rinaldi L, Alvarez Rojas CA, Torgerson PR, Harandi MF, Romig T, Antolova D, Schurer JM, Lahmar S, Cringoli G, Magambo J, Thompson RC, Jenkins EJ (2017) Global distribution of alveolar and cystic echinococcosis. Adv Parasit 95:315–493. https://doi.org/10.1016/bs.apar.2016.11.001
4. Trigui A, Toumi N, Fendri S, Saumtally MS, Zribi I, Akrout A, Mzali R, Ketata S, Dziri C, Amar MB, Boujelbene S (2024) Cystic echinococcosis of the liver: correlation between Intra-Operative ultrasound and Pre-Operative imaging. Surg Infect 25:213–220. https://doi.org/10.1089/sur.2023.335
5. Siles-Lucas M, Casulli A, Cirilli R, Carmena D (2018) Progress in the Pharmacological treatment of human cystic and alveolar echinococcosis: compounds and therapeutic targets. PLoS Negl Trop Dis 12:e0006422. https://doi.org/10.1371/journal.pntd.0006422
6. Mihmanli M, Idiz UO, Kaya C, Demir U, Bostanci O, Omeroglu S, Bozkurt E (2016) Current status of diagnosis and treatment of hepatic echinococcosis. World J Hepatol 8:1169. https://doi.org/10.4254/wjh.v8.i28.1169
7. Kajander EO, Ciftçioglu N (1998) Nanobacteria: an alternative mechanism for pathogenic intra-and extracellular calcification and stone formation. Proc Natl Acad Sci U S A 95:8274–8279. https://doi.org/10.1073/pnas.95.14.8274
8. Wang S, Yang L, Bai G, Gu Y, Fan Q, Guan X, Yuan J, Liu J (2024) A preliminary study on calcifying nanoparticles in dental plaque: isolation, characterization, and potential mineralization mechanism. Clin Exp Dent Res 10:e885. https://doi.org/10.1002/cre2.885. -n/a
9. He Z, Jing Z, Jing-Cun Z, Chuan-Yi H, Fei G (2017) Compositional analysis of various layers of upper urinary tract stones by infrared spectroscopy. Exp Ther Med 14:3165–3169. https://doi.org/10.3892/etm.2017.4864
10. Jun ZM, Hong FC, Chun ZD (2015) The cytotoxic effect of nanobacteria on human osteoblast cells. 14–18
11. Das S, Shukla N, Singh SS, Kushwaha S, Shrivastava R (2021) Mechanism of interaction between autophagy and apoptosis in cancer. Apoptosis 26:1–22. https://doi.org/10.1007/s10495-021-01687-9
12. Nicolao MC, Loos JA, Rodriguez Rodrigues C, Beas V, Cumino AC (2017) Bortezomib initiates Endoplasmic reticulum stress, elicits autophagy and death in *Echinococcus granulosus* larval stage. PLoS ONE 12:e0181528. https://doi.org/10.1371/journal.pone.0181528
13. Loos JA, Cumino AC (2015) In vitro anti-echinococcal and metabolic effects of Metformin involve activation of AMP-activated protein kinase in larval stages of *Echinococcus granulosus*. PLoS ONE 10:e0126009. https://doi.org/10.1371/journal.pone.0126009
14. Kajander EO, Ciftcioglu N, Aho K, Garcia-Cuerpo E (2003) Characteristics of nanobacteria and their possible role in stone formation. Urol Res 31:47–54. https://doi.org/10.1007/s00240-003-0304-7
15. Liu X, Chen J, Zhu YS, JI MY, Chen CM, Chen KF, SU HW (2020) Mechanism of autophagy on the formation of kidney stones caused by calcified nanoparticles. J Med Postgrad 2020:44–49
16. Wang Z, Zhang Y, Zhang J, Deng Q, Liang H (2021) Recent advances on the mechanisms of kidney stone formation. Int J Mol Med 48:149. https://doi.org/10.3892/ijmm.2021.4982
17. Kang T, Mao H, Lin J, Zhu T, Zhang L, Zhang D, Wu W, Ou S (2023) Effects of autophagy on vascular calcification in chronic kidney disease. Chin J Compar Med 3:51–60
18. Yang J, Peng X, Zhang H, Yang J, Zhang Y, Wu X (2022) Isolation culture and morphological observation of calcifying nanoparticles in the pericyst wall of hepatic hydatid cyst. J Shihezi University(Natural Science) 38:507–512
19. Yaghobee S, Bayani M, Samiei N, Jahedmanesh N (2015) What are the nanobacteria? Biotechnol Biotec Eq. 29:826–833
20. Yang J, Wang M, Chu Z, Zhang Y, Yang J, Chen X, Wu X, Peng X (2022) Role of calcified nanoparticles in the calcification of cystic hepatic hydatid in Northern xinjiang, china: a preliminary study. Acta Med Mediterr 1335–1346
21. Liu J, Gao J, Liang Z, Gao C, Niu Q, Wu F, Zhang L (2022) Mesenchymal stem cells and their microenvironment. Stem Cell Res Ther 13:429. https://doi.org/10.1186/s13287-022-02985-y
22. Woolsey ID, Miller AL (2021) *Echinococcus granulosus* sensu Lato and Echinococcus multilocularis: A review. Res Vet Sci 135:517–522. https://doi.org/10.1016/j.rvsc.2020.11.010
23. Conchedda M, Caddori A, Caredda A, Capra S, Bortoletti G (2018) Degree of calcification and cyst activity in hepatic cystic echinococcosis in humans. Acta Trop 182:135–143. https://doi.org/10.1016/j.actatropica.2018.02.027
24. Hunter LW, Charlesworth JE, Yu S, Lieske JC, Miller VM (2014) Calcifying nanoparticles promote mineralization in vascular smooth muscle cells: implications for atherosclerosis. Int J Nanomed 9:2689–2698. https://doi.org/10.2147/IJN.S63189
25. Ma B, Cao W, Li W, Gao C, Qi Z, Zhao Y, Du J, Xue H, Peng J, Wen J, Chen H, Ning Y, Huang L, Zhang H, Gao X, Yu L, Chen YG (2014) Dapper1 promotes autophagy by enhancing the Beclin1-Vps34-Atg14L complex formation. Cell Res 24:912–924
26. Kang R, Zeh HJ, Lotze MT, Tang D (2011) The Beclin 1 network regulates autophagy and apoptosis. Cell Death Differ 18:571–580. https://doi.org/10.1038/cdd.2010.191
27. Xie Y, Kang R, Tang D (2016) Role of the Beclin 1 network in the cross-regulation between autophagy and apoptosis. Autophagy: cancer, other pathologies, inflammation, immunity, infection, and aging. Elsevier, pp 75–88
28. Mei Y, Glover K, Su M, Sinha SC (2016) Conformational flexibility of BECN1: essential to its key role in autophagy and beyond. Protein Sci 25:1767–1785. https://doi.org/10.1002/pro.2984
29. Holah NS, El-Dien MMS, Mahmoud SF (2022) Expression of autophagy markers Beclin1 and LC3B in prostatic carcinoma: an

immunohistochemical case-control study. Iran J Pathol 17:75. https://doi.org/10.30699/IJP.2021.530887.2649
30. Zhou X, Xu SN, Yuan ST, Lei X, Sun X, Xing L, Li HJ, He CX, Qin W, Zhao D, Li PQ, Moharomd E, Xu X, Cao HL (2021) Multiple functions of autophagy in vascular calcification. Cell Biosci 11:1–14. https://doi.org/10.1186/s13578-021-00639-9
31. Klionsky DJ, Petroni G, Amaravadi RK et al (2021) Autophagy in major human diseases. EMBO J 40:e108863. https://doi.org/10.15252/embj.2021108863
32. Wu Chengwen 2019 AGEs induce autophagy and promote calcification of human aortic smooth muscle cells (Master's thesis, Southwest Medical University)